

Part Ie. Radio Recombination Lines

Recombination line masers in YSOs

Jesús Martín-Pintado

*Observatorio Astronómico Nacional (IGN), Campus Universitario,
Apartado 1143, E-28800 Alcalá de Henares, Spain*

Abstract. Maser emission from recombination lines has been detected towards the Young Stellar Object (YSO) MWC349 and the massive evolved star η Carinae. In spite of extensive searches of recombination line maser emission at millimeter wavelengths towards massive star forming regions, MWC349 remains unique. MWC349 is also a strong recombination line laser in the Far-IR with the largest amplification observed for transitions at wavelengths around 400 μm . The observational properties of the recombination line maser and laser emission from MWC349 are reviewed. Modeling of the maser and laser emission in MWC349 will be used to illustrate the potential of this kind of masers to understand the early phases of the evolution of massive stars. The impact that future instruments like the Herschel, the SMA and specially ALMA, will have in the investigation of recombination line maser emission from YSOs is briefly discussed.

1. Introduction

Radio recombination lines (RLs) were first discovered in interstellar space by Dravskikh & Dravskikh (1964). Soon after, Goldberg (1965) showed that recombination lines at centimeter wavelengths were expected to be formed in non-LTE (Local Thermodynamic Equilibrium) and stimulated emission must occur. The extent to which non-LTE effects influence the line intensities of the radio RLs has been subject of debate in the last two decades (see e.g. Roelfsema & Goss 1992). The most accepted idea is that RLs at wavelengths longer than 1 cm arising in conventional galactic HII regions are emitted under near-LTE conditions and stimulated emission is not very important. At millimeter wavelengths, the expected stimulated emission in the RLs arising from typical galactic HII regions is also negligible (Walmsley 1980).

After 25 years of research on RLs, strong time variable maser emission was first detected toward the massive the YSO MWC349 in the RLs H29 α , H30 α and H31 α at wavelengths of ~ 1.3 mm (Martín-Pintado et al. 1989a; Martín-Pintado, Bachiller & Thum 1989b; Thum, Martín-Pintado & Bachiller 1992). Today, maser emission in MWC349 has been observed for recombination lines with quantum number, n , between 10 and 35 (i. e. wavelength between 25 μm and 2 mm) (Thum et al. 1994a,b; Strel'nitski et al. 1996a; Thum et al. 1998). Extensive searches for RL masers carried out towards other YSOs in regions of massive star formation at mm and submm wavelengths have been unsuccessful. So far, MWC 349 remains the only known YSO which shows maser emission in

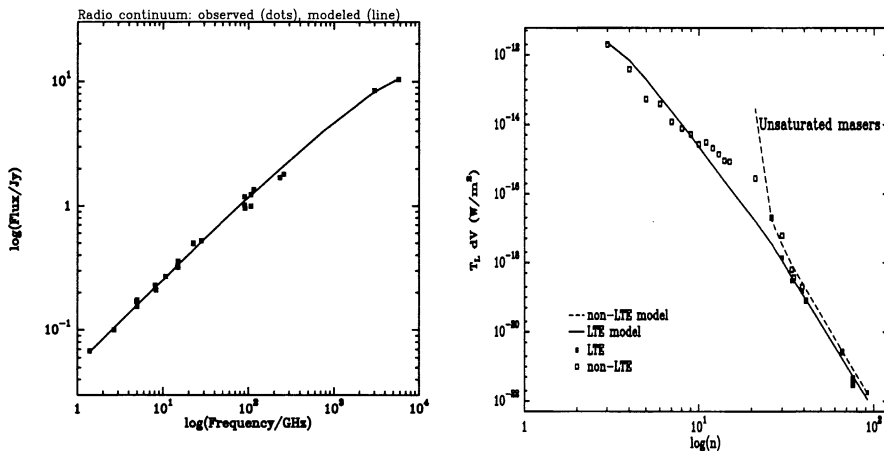


Figure 1. **a** (left panel) Continuum spectrum of MWC349 (filled squares, Harvey et al. 1979). The solid line shows the model prediction (section 4). **b** (right panel) Integrated line intensity of the measured RLs as a function of quantum number (squares, Thum et al. 1998). Model predictions (section 4) for thermal (solid line) and non-LTE –maser– (dashed lines) emission are shown.

RLs. In fact, the second source where RL maser emission has been detected is the evolved massive star η Carinae (Cox et al. 1995). This article will concentrate only on the Hydrogen α ($\Delta n=1$) RL emission from MWC349. RL emission from η Carinae will be discussed in detail by Abraham & Damiani (this volume).

2. Recombination line masers

The presence of strong RL maser emission at mm, submm and Far-IR wavelengths does not seem to be related to the nature of the sources, but to the structure and the kinematics of the ionized gas. The two sources with RL masers show a power law continuum spectrum, $S_\nu \sim \nu^\gamma$ with $\gamma > 0$, typical of an isothermal ionized stellar wind. Fig. 1a shows the continuum spectrum of MWC349 from $100 \mu\text{m}$ up to 21 cm . The value of γ for MWC349 is 0.64, indicating that the density varies with the radius, r , like $r^{-2.04}$ (Panagia & Felli 1975, Wright & Barlow 1975). The density gradient in η Carinae is steeper than for MWC349 with a density profile like $r^{-3.5}$. Because of the large density gradients in these HII regions, the densities in the inner parts can be higher than 10^6 cm^{-3} . For such a large electron densities the population of the level involved in the RLs at mm and submm wavelengths are inverted and the line opacities can be negative (Walmsley 1990; Strelitski et al. 1996b). At cm wavelengths, RLs are optically thin because the free-free continuum opacity is always larger than the RLs opacities. However, at wavelengths around 3 mm, the RL opacities are larger than the continuum opacities and RLs at wavelengths shorter than 3 mm are optically thick. Then, high gain RL masers with optical depths < -1 can only be observed for RLs with $n < 40$ (Martín-Pintado et al. 1989a). RL emission at

cm wavelengths from ionized stellar winds is not expected to show high gain masers, but stimulated emission (Martín-Pintado et al. 1993).

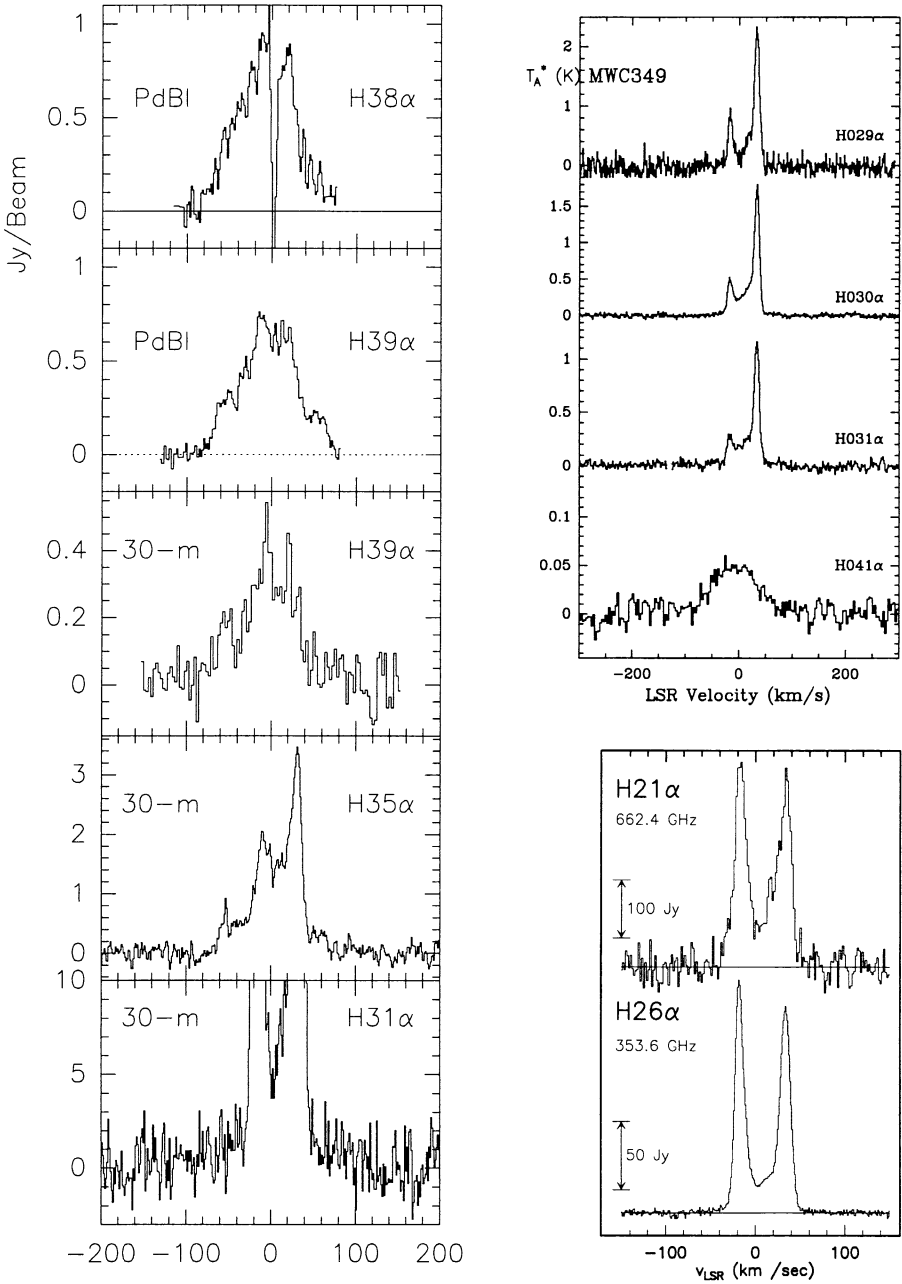


Figure 2. Sample of RL profiles at mm and submm wavelengths taken towards MWC349 (Martín-Pintado et al. 1989a, 1994; Thum et al. 1994a, 1994b)

3. Properties of the RL emission in MWC349

Basically all RLs arising from MWC349 have been observed from cm wavelengths to the visible. One of the most interesting aspects of the different type of the RL emission (LTE, stimulated and high gain maser emission) observed in MWC349 is that it seems to be associated with the different components of the ionized gas. High angular resolution images at cm wavelengths of the radio continuum emission show a biconical surface distribution of ionized gas (Cohen et al. 1985). The morphology of the ionized material in MWC349 can be explained by two components: a very dense, edge-on, neutral circumstellar disk and an ionized bipolar wind (Cohen et al. 1985). Three different types of RL emission have been detected so far: a) LTE and stimulated emission, b) low-velocity high gain masers (LVHGMs), and c) high-velocity masers (HVMs). Fig. 2 shows a sample of profiles for RLs at mm and submm wavelengths. We will briefly discuss the different types of RL emission in MWC349.

3.1. LTE and stimulated emission (bipolar wind)

The RLs from this component were first detected at cm wavelengths by Altenhoff et al. (1981). The line intensities were consistent with LTE emission and showed broad (90 km s^{-1}) gaussian profiles. This component has been observed in several RLs with wavelengths from 1.3 mm to 3 cm (Altenhoff et al. 1981; Martín-Pintado et al. 1989a,1993,1994; Escalante et al. 1989; Rodriguez et al. 1992; Thum et al. 1992; Gordon 1992). The spectrum of the $\text{H}41\alpha$ in Fig 2 shows the typical line profile of this component. The lack of time variability of the $\text{H}41\alpha$ line also supports the idea of LTE emission for these lines (Thum et al. 1992). Although most of the intensities and profiles (symmetric) of the RLs with $n > 40$ observed with single dish are consistent with LTE emission, the intensities and the profiles (asymmetric) observed with interferometers indicates that stimulated emission is important towards the strongest continuum peaks (Martín-Pintado et al. 1993,1994). High angular resolution observation of RLs show that this component arises from the ionized bipolar wind expanding at a constant velocity of 58 km s^{-1} (Martín-Pintado et al.1993; Rodriguez et al. 1992).

3.2. Low velocity masers & IR lasers (interface disk-wind)

In contrast with the broad nearly gaussian profiles observed in the RLs with $n > 40$, the RLs with $n < 30$ show two time variable high gain maser spikes at radial velocities of ~ -15 and $\sim 30 \text{ km s}^{-1}$. The maser spikes (hereafter low-velocity high gain masers LVHGMs) has now been observed for RLs with n between 21 and 35 (Martín-Pintado et al. 1989a,b; Gordon 1992; Thum et al. 1994a,b). Fig 2 shows a collection of RL lines profiles which illustrates that strong amplification in the LVHGMs sets for $n \sim 35$. Observations of the integrated intensity of the IR RLs with the KAO and ISO show that maser amplification takes place for RLs with n down to ~ 10 (Strelitski et al. 1996a; Thum et al. 1998). Fig. 1b shows the integrated intensity of all RLs measured up to date. The solid line shows the expected LTE emission from the model described in section 4. The high gain RL masers/lasers in MWC349 take place for $10 < n < 37$ with the largest maser gain for RLs in the submm range ($n \sim 20$).

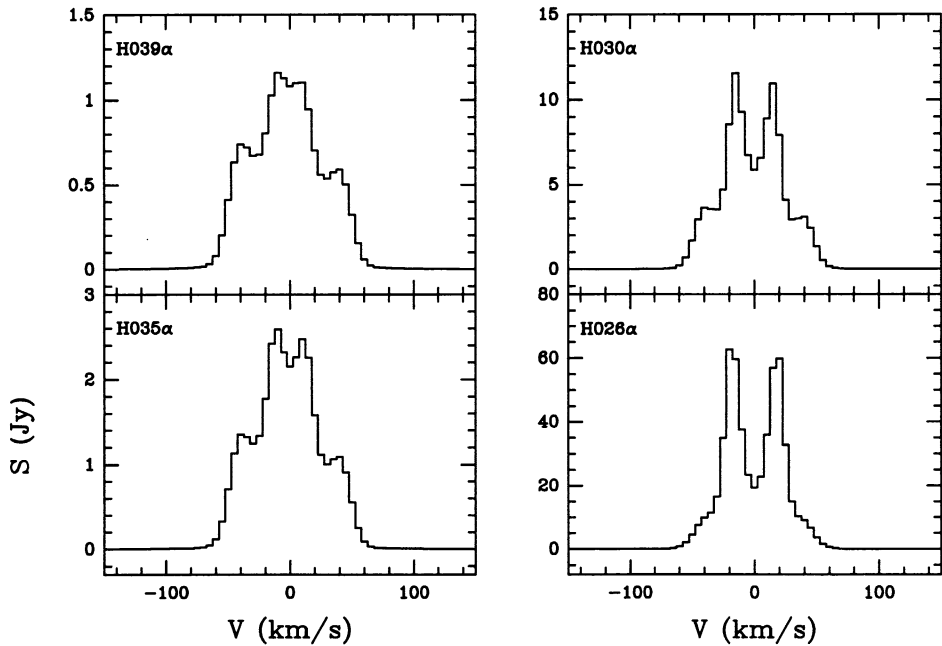


Figure 3. Sample of RL profiles predicted by the model for the case of non-LTE emission

Interferometric observations of the maser spikes reveal that they originate from two positions separated by 80 AU associated with the ionized edges of a neutral nearly edge-on disk (Planesas, Martín-Pintado & Serabyn 1992). The systematic trend of the velocity separation of the two peaks (increasing from the H39 α to H26 α) is consistent with the hypothesis that the LVHGMs arises from the ionized skins of an edge-on, gravitationally bound circumstellar disk rotating with a Keplerian law (Hamman & Simon 1986). However, the radial velocity separation of the LVHGMs for the H21 α deviates from that expected in Keplerian rotation. Recently, Thum & Morris (1999) have reported the detection of the Zeeman splitting in the LVHGMs. They inferred a magnetic field in the disk of 22 mG. The detection of the magnetic field in the disk of MWC349 can help to understand whether, as suggested by Hamman & Simon (1986), the disk is the source of the bipolar flow of ionized gas.

3.3. High velocity masers (bipolar wind but close to the disk)

In addition to the LVHGMs, some RLs like the H35 α and the H39 α (see Fig. 2) also show narrow features (width of 15–20 km s⁻¹) at radial velocities of -58 and 58 km s⁻¹, close to the terminal velocity of the bipolar ionized wind. These features are time variable and their intensities indicates maser emission (Martín-Pintado et al 1994). These high-velocity masers (HVMs) also appear when one compares the profiles of the H21 α and H26 α lines (Thum et al. 1994a). It has been proposed that HVMs arise from the interface region of the ionized stellar wind and the neutral disk (Martín-Pintado et al 1994).

4. The nature of MWC349

MWC349 can be used as a laboratory to test the RL maser & laser theory. Furthermore, one can use the large observational set of RLs and radio continuum images to understand the nature of this ultracompact HII (UCHII) region. This is important in order to understand the evolution of young massive stars since there is increasing evidence that a substantial minority of UCHII regions have properties similar to those of MWC349 (Jaffe & Martín-Pintado 1999). These kind of UCHII regions (known as BRLOs) are compact (< 0.04 pc) show broad ($70\text{--}100$ km s $^{-1}$) RLs and continuum power law spectra with an index, γ , between 0.6 and 1. It has been proposed that the long life time of the UCHII regions such as MWC349 and the BRLOs could be explained by photoevaporated disks (Hollenbach et al. 1994; Gaume et al. 1995; Jaffe & Martín-Pintado 1999). However, detailed modeling to explain the RL and continuum emission arising from MWC349 in the framework of a photoevaporated disk has not been made so far. Most of the models have addressed particular aspects of the RL emission in MWC349 under some assumptions (Martín-Pintado et al 1993, Strel'nitski et al. 1996b, 1996c).

Martín-Pintado et al (1993) has considered a radiative transfer model to predict the continuum and the RL emissions for both LTE and non-LTE conditions using a photoevaporated disk model (Hollenbach et al 1994). Martín-Pintado, Planesas & Thum (2001) have extended the previous model by considering Keplerian rotation for a thin ionized layer on the surface of the neutral disk.

The main results of the model for the RLs and continuum emissions are shown in Figs. 1a, 1b and 3. The model fits the continuum spectrum for the whole frequency range (see solid line in Fig. 1a) and the continuum morphology at 23 GHz (see Martín-Pintado et al. 1993). This indicates that the simple density law used in this model describes the density distribution even at scales smaller than a few AUs. The solid line in Fig. 1b shows the predicted integrated line intensities of the RLs for thermal emission with the level population derived by Walmsley (1990) and Storey & Hummer (1995). The predicted thermal line intensities are in good agreement for the RLs with $35 < n < 10$. The discrepancies found for some of the RLs at cm wavelengths, such as the H66 α line observed with interferometers, can be explained when stimulated emission is considered (see dashed line in Fig. 1b).

The integrated intensity of the RLs with LVHGMs ($10 < n < 35$) is obviously much larger than the predicted thermal emission. The model prediction for the case of non-LTE emission –maser amplification–, shown as dashed lines in Fig. 1b, are in agreement with the observed integrated intensities of RLs with $n > 26$. For $n < 26$, the predicted line intensities are much larger than those measured. This is likely due to the fact that the model does not consider the saturation effect in the maser. Thum et al. (1994b) and Strel'nitski et al. (1996b) have argued that the LVHGMs are saturated for RLs with $n < 26$. Models that consider the effects of the maser radiation on the level population confirm that saturation effects are very important even in the case of a thin layer geometry (Hengel & Kegel 2000). Then, to properly account for the intensities and line profiles of LVHGMs in MWC349 for RLs with $n < 26$ the models must consider saturation effects.

A sample of the predicted line profiles of selected RLs when non-LTE emission is considered is shown in Fig. 3. The predicted profiles are in relatively good agreement with the measured ones (see Fig.2). The model predicts the two kinds of masers observed in MWC349, the LVHGMs and the HVMs. The radial velocities and linewidths of both types of masers as well as the increase of the velocity separation between the spikes of the HVHGMs are well reproduced by the model for the RLs with $n > 26$. The predicted velocity separation for the HVHGMs in the H21 α line is much larger than the observed one. This would indicate that in inner parts of the disk are not rotating with a Keplerian law. However, saturation effects and/or density fluctuations in the disk could also explain the profile of the H21 α line. Models which take into account the saturation effects of the Far-IR lasers are needed in order to establish the kinematics in the inner parts of the disk in MWC349.

5. Future prospects

There are a number of future instruments working in the mm, submm and Far-IR wavelengths like the Herschel, the Submillimeter Array (SMA) and Atacama Large Millimeter Array (ALMA) with the potential to make a significant change in the research of RL masers & lasers. For the already known RL maser sources, MWC349 and η Carinae, the SMA will be able to obtain information on the relative location of the maser spots in the RLs at submm wavelengths, and ALMA will map both sources in great detail in many RLs and in the continuum. Masers spots will likely be resolved for baselines larger than 3 km. Finally, HIFI onboard the Herschel will provide line profiles of all RLs up to 1.7 THz ($n > 15$) in both sources. All the instruments will provide the possibility of detecting and studying in great detail new RL maser & IR laser sources. In particular, the BRLOs are excellent candidates for RL maser/laser emitters.

Acknowledgments. This work has been partially supported by the PNIE and the European Commission under grant number 1FD1997-1442. We thank P. Planesas for the reading of the manuscript.

References

- Altenhoff, W. J., Strittmatter, P. A., Wendker, H. J. 1981, *A&A*, 93, 48
 Cohen, M., Bieging, J.H., Dreher, J.W. & Welch, W.J. 1985, *ApJ*, 292, 249
 Cox, P., Martín-Pintado, J., Bachiller, R., Bronfman, L., Cernicharo, J., Nyman, L., Roelfsema, P.R. 1995 *A&A*, 295L, 39
 Dravskikh, Z. V. & Dravskikh, A. F. 1964, *Astron. Tsirk.*, 158, 2
 Escalante, V., Rodriguez, L.F., Moran, J.M. & Cantó, J. 1989, *Rev. Mexicana Astron. Astrof.*, 17, 11
 Gaume, R. A., Goss, W. M., Dickel, H. R., Wilson, T. L. & Johnston, K.J. 1995, *ApJ*, 438, 776
 Goldberg, L 1966, *ApJ*, 144,1225
 Gordon, M. 1992, *ApJ*, 387, 701
 Hamman, F. & Simon, M. 1986, *ApJ*, 311, 909

- Harvey, P.M., Thronson, H.A. & Gatley, I. 1979, *ApJ*, 233, 115
- Hengel, C. & Kegel, W.H. 2000, *A&A*, 361, 1169
- Hollenbach, D., Johnstone, D., Lizano, S., & Shu, F. 1994, *ApJ*, 428, 654
- Jaffe, D.T. & Martín-Pintado, J. 1999, *ApJ*, 520, 162
- Martín-Pintado, J., Bachiller, R., Thum C. & Walmsley, M.C. 1989a, *A&A*, 215, L13
- Martín-Pintado, Thum, C. & Bachiller, R. 1989b, *A&A*, 229, L9
- Martín-Pintado, Gaume, R., Bachiller, R., Johnston, K. & Planesas, P. 1993, *ApJL*, 418, 79
- Martín-Pintado, J, Neri, R., Thum, C., Planesas P. & Bachiller, R. 1994, *A&A*, 286, 890
- Martín-Pintado, J., Planesas, P., & Thum, C. 2001, in preparation
- Panagia, N., Felli, N. 1975, *A&A*, 39, 1
- Planesas, P., Martín-Pintado, J. & Serabyn, E. 1992, *ApJL*, 386, L23
- Rodriguez, L.F. & Bastian, T.S. 1992, 2nd ESO/CTIO Workshop on "Mass Loss on the AGB and Beyond", De. ESO
- Roelfsema, P.R. & Goss, W.M., 1992, *A&AR*, 4, 161 Storey, P.J. & Hummmer, D.G. 1995, *MNRAS*, 272, 41
- Strelitski, V. , Haas, M.. R., Smith, H. A., Erickson, E. F., Colgan, S. W. J. & Hollenbach, D.J. 1996a, *Science*, 272, 1459
- Strelitski, V. S., Ponomarev, V.O. & Smith, H. A. 1996b, *ApJ*, 470, 1118
- Strelitski, V. S., Smith, H. A. & Ponomarev, V. O. 1996c, *ApJ*, 470, 1134
- Thum, C. Martín-Pintado, J. & Bachiller, R. 1992, *A&A*, 256, 507
- Thum, C., Matthews, H. E., Harris, A.I., Tacconi, L.J., Schuster, K.F. & Martín-Pintado, J. 1994a, *A&A*, 288L, 25
- Thum, C., Matthews, H.E., Martín-Pintado, J., Serabyn, E., Planesas, P. & Bachiller, R. 1994b, *A&A*, 283, 582
- Thum, C., Martín-Pintado, J., Quirrenbach, A. & Matthews, H. E. 1998, *A&A*, 333L, 63
- Thum, C., Morris, D. 1999, *A&A*, 344, 923
- Walmley C. M.: 1980, in *Radio Recombination Lines*, ed. P. Shaver, Reidel Company, p. 37
- Walmsley, C.M. 1990, *A&AS*, 82, 201
- White, R.L. and Becker, R.H. 1985, *ApJ*, 297, 677
- Wright, A.E., Barlow, M.J. 1975, *MNRAS*, 170, 41

Recombination line masers in YSOs

Jesús Martín-Pintado

*Observatorio Astronómico Nacional (IGN), Campus Universitario,
Apartado 1143, E-28800 Alcalá de Henares, Spain*

Abstract. Maser emission from recombination lines has been detected towards the Young Stellar Object (YSO) MWC349 and the massive evolved star η Carinae. In spite of extensive searches of recombination line maser emission at millimeter wavelengths towards massive star forming regions, MWC349 remains unique. MWC349 is also a strong recombination line laser in the Far-IR with the largest amplification observed for transitions at wavelengths around 400 μm . The observational properties of the recombination line maser and laser emission from MWC349 are reviewed. Modeling of the maser and laser emission in MWC349 will be used to illustrate the potential of this kind of masers to understand the early phases of the evolution of massive stars. The impact that future instruments like the Herschel, the SMA and specially ALMA, will have in the investigation of recombination line maser emission from YSOs is briefly discussed.

1. Introduction

Radio recombination lines (RLs) were first discovered in interstellar space by Dravskikh & Dravskikh (1964). Soon after, Goldberg (1965) showed that recombination lines at centimeter wavelengths were expected to be formed in non-LTE (Local Thermodynamic Equilibrium) and stimulated emission must occur. The extent to which non-LTE effects influence the line intensities of the radio RLs has been subject of debate in the last two decades (see e.g. Roelfsema & Goss 1992). The most accepted idea is that RLs at wavelengths longer than 1 cm arising in conventional galactic HII regions are emitted under near-LTE conditions and stimulated emission is not very important. At millimeter wavelengths, the expected stimulated emission in the RLs arising from typical galactic HII regions is also negligible (Walmsley 1980).

After 25 years of research on RLs, strong time variable maser emission was first detected toward the massive the YSO MWC349 in the RLs H29 α , H30 α and H31 α at wavelengths of ~ 1.3 mm (Martín-Pintado et al. 1989a; Martín-Pintado, Bachiller & Thum 1989b; Thum, Martín-Pintado & Bachiller 1992). Today, maser emission in MWC349 has been observed for recombination lines with quantum number, n , between 10 and 35 (i. e. wavelength between 25 μm and 2 mm) (Thum et al. 1994a,b; Strel'nitski et al. 1996a; Thum et al. 1998). Extensive searches for RL masers carried out towards other YSOs in regions of massive star formation at mm and submm wavelengths have been unsuccessful. So far, MWC 349 remains the only known YSO which shows maser emission in

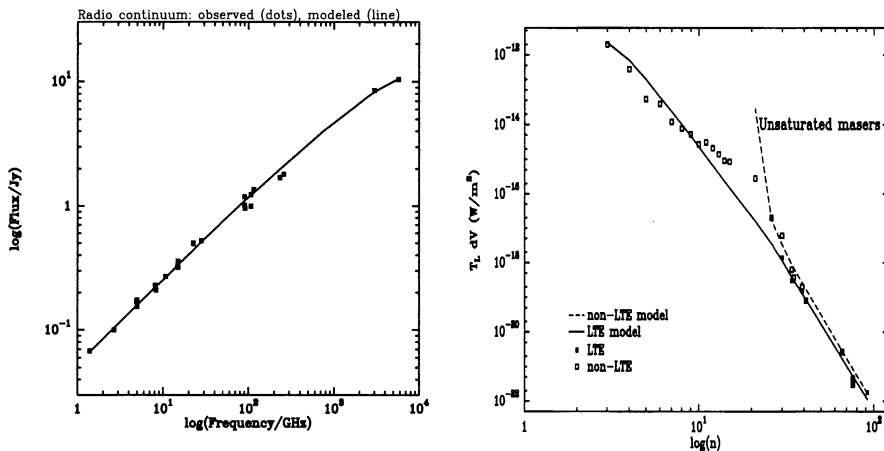


Figure 1. **a** (left panel) Continuum spectrum of MWC349 (filled squares, Harvey et al. 1979). The solid line shows the model prediction (section 4). **b** (right panel) Integrated line intensity of the measured RLs as a function of quantum number (squares, Thum et al. 1998). Model predictions (section 4) for thermal (solid line) and non-LTE –maser– (dashed lines) emission are shown.

RLs. In fact, the second source where RL maser emission has been detected is the evolved massive star η Carinae (Cox et al. 1995). This article will concentrate only on the Hydrogen α ($\Delta n=1$) RL emission from MWC349. RL emission from η Carinae will be discussed in detail by Abraham & Damineli (this volume).

2. Recombination line masers

The presence of strong RL maser emission at mm, submm and Far-IR wavelengths does not seem to be related to the nature of the sources, but to the structure and the kinematics of the ionized gas. The two sources with RL masers show a power law continuum spectrum, $S_\nu \sim \nu^\gamma$ with $\gamma > 0$, typical of an isothermal ionized stellar wind. Fig. 1a shows the continuum spectrum of MWC349 from 100 μm up 21 cm. The value of γ for MWC349 is 0.64, indicating that the density varies with the radius, r , like $r^{-2.04}$ (Panagia & Felli 1975, Wright & Barlow 1975). The density gradient in η Carinae is steeper than for MWC349 with a density profile like $r^{-3.5}$. Because of the large densities gradients in these HII regions, the densities in the inner parts can be higher than 10^6 cm^{-3} . For such a large electron densities the population of the level involved in the RLs at mm and submm wavelengths are inverted and the line opacities can be negative (Walmsley 1990; Strelitski et al. 1996b). At cm wavelengths, RLs are optically thin because the free-free continuum opacity is always larger than the RLs opacities. However, at wavelengths around 3 mm, the RL opacities are larger than the continuum opacities and RLs at wavelengths shorter than 3 mm are optically thick. Then, high gain RL masers with optical depths < -1 can only be observed for RLs with $n < 40$ (Martín-Pintado et al. 1989a). RL emission at

cm wavelengths from ionized stellar winds is not expected to show high gain masers, but stimulated emission (Martín-Pintado et al. 1993).

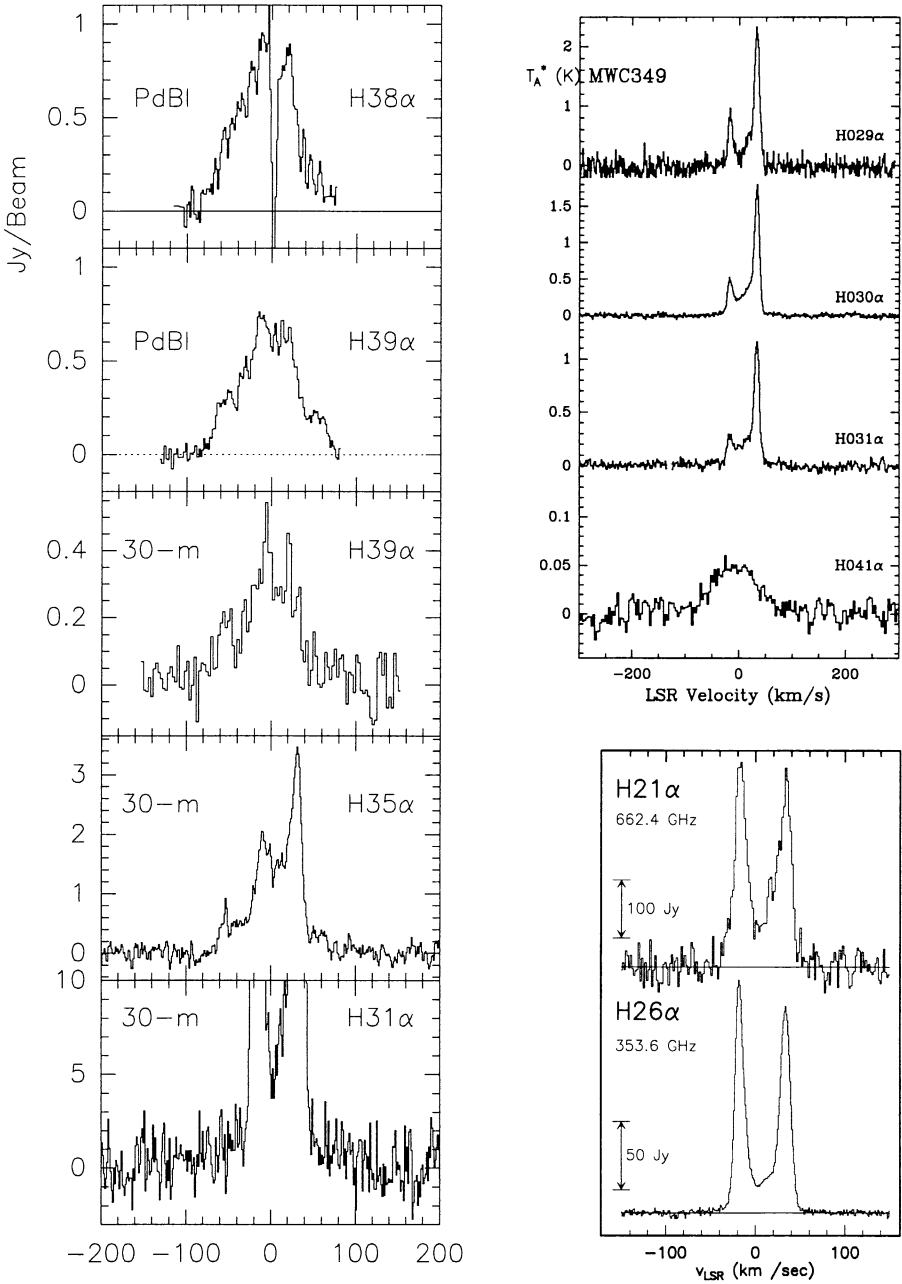


Figure 2. Sample of RL profiles at mm and submm wavelengths taken towards MWC349 (Martín-Pintado et al. 1989a, 1994; Thum et al. 1994a, 1994b)

3. Properties of the RL emission in MWC349

Basically all RLs arising from MWC349 have been observed from cm wavelengths to the visible. One of the most interesting aspects of the different type of the RL emission (LTE, stimulated and high gain maser emission) observed in MWC349 is that it seems to be associated with the different components of the ionized gas. High angular resolution images at cm wavelengths of the radio continuum emission show a biconical surface distribution of ionized gas (Cohen et al. 1985). The morphology of the ionized material in MWC349 can be explained by two components: a very dense, edge-on, neutral circumstellar disk and an ionized bipolar wind (Cohen et al. 1985). Three different types of RL emission have been detected so far: a) LTE and stimulated emission, b) low-velocity high gain masers (LVHGMs), and c) high-velocity masers (HVMs). Fig. 2 shows a sample of profiles for RLs at mm and submm wavelengths. We will briefly discuss the different types of RL emission in MWC349.

3.1. LTE and stimulated emission (bipolar wind)

The RLs from this component were first detected at cm wavelengths by Altenhoff et al. (1981). The line intensities were consistent with LTE emission and showed broad (90 km s^{-1}) gaussian profiles. This component has been observed in several RLs with wavelengths from 1.3 mm to 3 cm (Altenhoff et al. 1981; Martín-Pintado et al. 1989a,1993,1994; Escalante et al. 1989; Rodriguez et al. 1992; Thum et al. 1992; Gordon 1992). The spectrum of the $\text{H}41\alpha$ in Fig 2 shows the typical line profile of this component. The lack of time variability of the $\text{H}41\alpha$ line also supports the idea of LTE emission for these lines (Thum et al. 1992). Although most of the intensities and profiles (symmetric) of the RLs with $n > 40$ observed with single dish are consistent with LTE emission, the intensities and the profiles (asymmetric) observed with interferometers indicates that stimulated emission is important towards the strongest continuum peaks (Martín-Pintado et al. 1993,1994). High angular resolution observation of RLs show that this component arises from the ionized bipolar wind expanding at a constant velocity of 58 km s^{-1} (Martín-Pintado et al.1993; Rodriguez et al. 1992).

3.2. Low velocity masers & IR lasers (interface disk-wind)

In contrast with the broad nearly gaussian profiles observed in the RLs with $n > 40$, the RLs with $n < 30$ show two time variable high gain maser spikes at radial velocities of ~ -15 and $\sim 30 \text{ km s}^{-1}$. The maser spikes (hereafter low-velocity high gain masers LVHGMs) has now been observed for RLs with n between 21 and 35 (Martín-Pintado et al. 1989a,b; Gordon 1992; Thum et al. 1994a,b). Fig 2 shows a collection of RL lines profiles which illustrates that strong amplification in the LVHGMs sets for $n \sim 35$. Observations of the integrated intensity of the IR RLs with the KAO and ISO show that maser amplification takes place for RLs with n down to ~ 10 (Strelitski et al. 1996a; Thum et al. 1998). Fig. 1b shows the integrated intensity of all RLs measured up to date. The solid line shows the expected LTE emission from the model described in section 4. The high gain RL masers/lasers in MWC349 take place for $10 < n < 37$ with the largest maser gain for RLs in the submm range ($n \sim 20$).

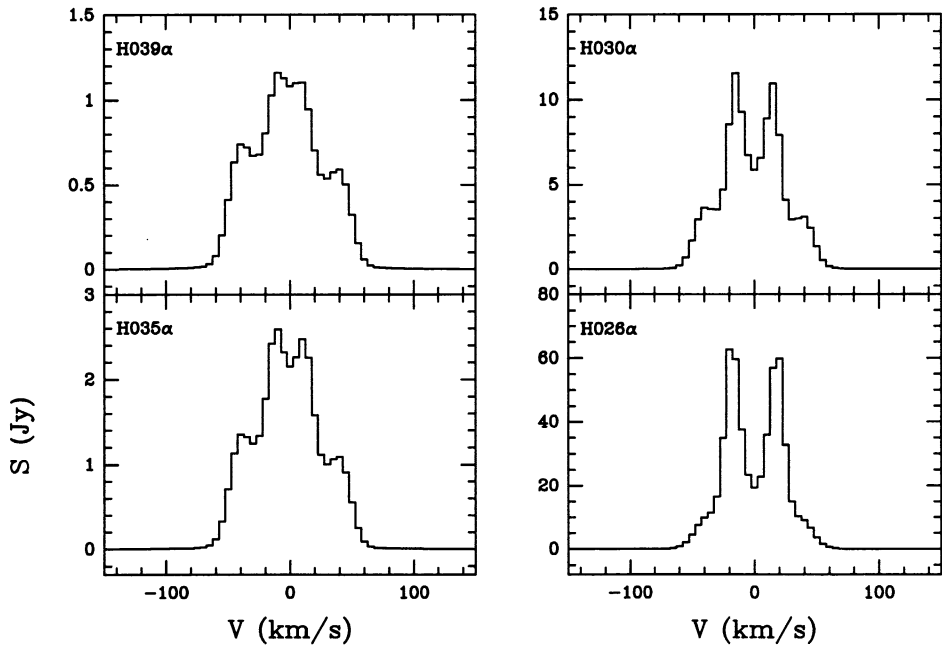


Figure 3. Sample of RL profiles predicted by the model for the case of non-LTE emission

Interferometric observations of the maser spikes reveal that they originate from two positions separated by 80 AU associated with the ionized edges of a neutral nearly edge-on disk (Planesas, Martín-Pintado & Serabyn 1992). The systematic trend of the velocity separation of the two peaks (increasing from the H39 α to H26 α) is consistent with the hypothesis that the LVHGMs arises from the ionized skins of an edge-on, gravitationally bound circumstellar disk rotating with a Keplerian law (Hamman & Simon 1986). However, the radial velocity separation of the LVHGMs for the H21 α deviates from that expected in Keplerian rotation. Recently, Thum & Morris (1999) have reported the detection of the Zeeman splitting in the LVHGMs. They inferred a magnetic field in the disk of 22 mG. The detection of the magnetic field in the disk of MWC349 can help to understand whether, as suggested by Hamman & Simon (1986), the disk is the source of the bipolar flow of ionized gas.

3.3. High velocity masers (bipolar wind but close to the disk)

In addition to the LVHGMs, some RLs like the H35 α and the H39 α (see Fig. 2) also show narrow features (width of 15–20 km s⁻¹) at radial velocities of -58 and 58 km s⁻¹, close to the terminal velocity of the bipolar ionized wind. These features are time variable and their intensities indicates maser emission (Martín-Pintado et al 1994). These high-velocity masers (HVMs) also appear when one compares the profiles of the H21 α and H26 α lines (Thum et al. 1994a). It has been proposed that HVMs arise from the interface region of the ionized stellar wind and the neutral disk (Martín-Pintado et al 1994).

4. The nature of MWC349

MWC349 can be used as a laboratory to test the RL maser & laser theory. Furthermore, one can use the large observational set of RLs and radio continuum images to understand the nature of this ultracompact HII (UCHII) region. This is important in order to understand the evolution of young massive stars since there is increasing evidence that a substantial minority of UCHII regions have properties similar to those of MWC349 (Jaffe & Martín-Pintado 1999). These kind of UCHII regions (known as BRLOs) are compact (< 0.04 pc) show broad ($70\text{--}100$ km s $^{-1}$) RLs and continuum power law spectra with an index, γ , between 0.6 and 1. It has been proposed that the long life time of the UCHII regions such as MWC349 and the BRLOs could be explained by photoevaporated disks (Hollenbach et al. 1994; Gaume et al. 1995; Jaffe & Martín-Pintado 1999). However, detailed modeling to explain the RL and continuum emission arising from MWC349 in the framework of a photoevaporated disk has not been made so far. Most of the models have addressed particular aspects of the RL emission in MWC349 under some assumptions (Martín-Pintado et al 1993, Strel'nitski et al. 1996b, 1996c).

Martín-Pintado et al (1993) has considered a radiative transfer model to predict the continuum and the RL emissions for both LTE and non-LTE conditions using a photoevaporated disk model (Hollenbach et al 1994). Martín-Pintado, Planesas & Thum (2001) have extended the previous model by considering Keplerian rotation for a thin ionized layer on the surface of the neutral disk.

The main results of the model for the RLs and continuum emissions are shown in Figs. 1a, 1b and 3. The model fits the continuum spectrum for the whole frequency range (see solid line in Fig. 1a) and the continuum morphology at 23 GHz (see Martín-Pintado et al. 1993). This indicates that the simple density law used in this model describes the density distribution even at scales smaller than a few AUs. The solid line in Fig. 1b shows the predicted integrated line intensities of the RLs for thermal emission with the level population derived by Walmsley (1990) and Storey & Hummer (1995). The predicted thermal line intensities are in good agreement for the RLs with $35 < n < 10$. The discrepancies found for some of the RLs at cm wavelengths, such as the H66 α line observed with interferometers, can be explained when stimulated emission is considered (see dashed line in Fig. 1b).

The integrated intensity of the RLs with LVHGMs ($10 < n < 35$) is obviously much larger than the predicted thermal emission. The model prediction for the case of non-LTE emission –maser amplification–, shown as dashed lines in Fig. 1b, are in agreement with the observed integrated intensities of RLs with $n > 26$. For $n < 26$, the predicted line intensities are much larger than those measured. This is likely due to the fact that the model does not consider the saturation effect in the maser. Thum et al. (1994b) and Strel'nitski et al. (1996b) have argued that the LVHGMs are saturated for RLs with $n < 26$. Models that consider the effects of the maser radiation on the level population confirm that saturation effects are very important even in the case of a thin layer geometry (Hengel & Kegel 2000). Then, to properly account for the intensities and line profiles of LVHGMs in MWC349 for RLs with $n < 26$ the models must consider saturation effects.

A sample of the predicted line profiles of selected RLs when non-LTE emission is considered is shown in Fig. 3. The predicted profiles are in relatively good agreement with the measured ones (see Fig.2). The model predicts the two kinds of masers observed in MWC349, the LVHGMs and the HVMs. The radial velocities and linewidths of both types of masers as well as the increase of the velocity separation between the spikes of the HVHGMs are well reproduced by the model for the RLs with $n > 26$. The predicted velocity separation for the HVHGMs in the H21 α line is much larger than the observed one. This would indicate that in inner parts of the disk are not rotating with a Keplerian law. However, saturation effects and/or density fluctuations in the disk could also explain the profile of the H21 α line. Models which take into account the saturation effects of the Far-IR lasers are needed in order to establish the kinematics in the inner parts of the disk in MWC349.

5. Future prospects

There are a number of future instruments working in the mm, submm and Far-IR wavelengths like the Herschel, the Submillimeter Array (SMA) and Atacama Large Millimeter Array (ALMA) with the potential to make a significant change in the research of RL masers & lasers. For the already known RL maser sources, MWC349 and η Carinae, the SMA will be able to obtain information on the relative location of the maser spots in the RLs at submm wavelengths, and ALMA will map both sources in great detail in many RLs and in the continuum. Masers spots will likely be resolved for baselines larger than 3 km. Finally, HIFI onboard the Herschel will provide line profiles of all RLs up to 1.7 THz ($n > 15$) in both sources. All the instruments will provide the possibility of detecting and studying in great detail new RL maser & IR laser sources. In particular, the BRLOs are excellent candidates for RL maser/laser emitters.

Acknowledgments. This work has been partially supported by the PNIE and the European Commission under grant number 1FD1997-1442. We thank P. Planesas for the reading of the manuscript.

References

- Altenhoff, W. J., Strittmatter, P. A., Wendker, H. J. 1981, *A&A*, 93, 48
 Cohen, M., Bieging, J.H., Dreher, J.W. & Welch, W.J. 1985, *ApJ*, 292, 249
 Cox, P., Martín-Pintado, J., Bachiller, R., Bronfman, L., Cernicharo, J., Nyman, L., Roelfsema, P.R. 1995 *A&A*, 295L, 39
 Dravskikh, Z. V. & Dravskikh, A. F. 1964, *Astron. Tsirk.*, 158, 2
 Escalante, V., Rodriguez, L.F., Moran, J.M. & Cantó, J. 1989, *Rev. Mexicana Astron. Astrof.*, 17, 11
 Gaume, R. A., Goss, W. M., Dickel, H. R., Wilson, T. L. & Johnston, K.J. 1995, *ApJ*, 438, 776
 Goldberg, L 1966, *ApJ*, 144,1225
 Gordon, M. 1992, *ApJ*, 387, 701
 Hamman, F. & Simon, M. 1986, *ApJ*, 311, 909

- Harvey, P.M., Thronson, H.A. & Gatley, I. 1979, *ApJ*, 233, 115
- Hengel, C. & Kegel, W.H. 2000, *A&A*, 361, 1169
- Hollenbach, D., Johnstone, D., Lizano, S., & Shu, F. 1994, *ApJ*, 428, 654
- Jaffe, D.T. & Martín-Pintado, J. 1999, *ApJ*, 520, 162
- Martín-Pintado, J., Bachiller, R., Thum C. & Walmsley, M.C. 1989a, *A&A*, 215, L13
- Martín-Pintado, Thum, C. & Bachiller, R. 1989b, *A&A*, 229, L9
- Martín-Pintado, Gaume, R., Bachiller, R., Johnston, K. & Planesas, P. 1993, *ApJL*, 418, 79
- Martín-Pintado, J, Neri, R., Thum, C., Planesas P. & Bachiller, R. 1994, *A&A*, 286, 890
- Martín-Pintado, J., Planesas, P., & Thum, C. 2001, in preparation
- Panagia, N., Felli, N. 1975, *A&A*, 39, 1
- Planesas, P., Martín-Pintado, J. & Serabyn, E. 1992, *ApJL*, 386, L23
- Rodriguez, L.F. & Bastian, T.S. 1992, 2nd ESO/CTIO Workshop on "Mass Loss on the AGB and Beyond", De. ESO
- Roelfsema, P.R. & Goss, W.M., 1992, *A&AR*, 4, 161 Storey, P.J. & Hummmer, D.G. 1995, *MNRAS*, 272, 41
- Strelitski, V. , Haas, M.. R., Smith, H. A., Erickson, E. F., Colgan, S. W. J. & Hollenbach, D.J. 1996a, *Science*, 272, 1459
- Strelitski, V. S., Ponomarev, V.O. & Smith, H. A. 1996b, *ApJ*, 470, 1118
- Strelitski, V. S., Smith, H. A. & Ponomarev, V. O. 1996c, *ApJ*, 470, 1134
- Thum, C. Martín-Pintado, J. & Bachiller, R. 1992, *A&A*, 256, 507
- Thum, C., Matthews, H. E., Harris, A.I., Tacconi, L.J., Schuster, K.F. & Martín-Pintado, J. 1994a, *A&A*, 288L, 25
- Thum, C., Matthews, H.E., Martín-Pintado, J., Serabyn, E., Planesas, P. & Bachiller, R. 1994b, *A&A*, 283, 582
- Thum, C., Martín-Pintado, J., Quirrenbach, A. & Matthews, H. E. 1998, *A&A*, 333L, 63
- Thum, C., Morris, D. 1999, *A&A*, 344, 923
- Walmley C. M.: 1980, in *Radio Recombination Lines*, ed. P. Shaver, Reidel Company, p. 37
- Walmsley, C.M. 1990, *A&AS*, 82, 201
- White, R.L. and Becker, R.H. 1985, *ApJ*, 297, 677
- Wright, A.E., Barlow, M.J. 1975, *MNRAS*, 170, 41